JOURNAL OF ENDOUROLOGY
Volume 33, Number 10, October 2019

Pp. 787–792
DOI: 10.1089/end.2018.0886

Evaluation of Renal Stone Comminution and Injury by Burst Wave Lithotripsy in a Pig Model

Adam D. Maxwell, PhD,[1,2] Yak-Nam Wang, PhD,[2] Wayne Kreider, PhD,[2] Bryan W. Cunitz, MS,[2] Frank Starr, BS,[2] Donghoon Lee, PhD,[3] Yasser Nazari,[3] James C. Williams Jr., PhD,[4] Michael R. Bailey, PhD,[1,2] and Mathew D. Sorensen, MD, MS[1,5]

Abstract

Introduction: Burst wave lithotripsy is an experimental technology to noninvasively fragment kidney stones with focused bursts of ultrasound (US). This study evaluated the safety and effectiveness of specific lithotripsy parameters in a porcine model of nephrolithiasis.
Methods: A 6- to 7-mm human kidney stone was surgically implanted in each kidney of three pigs. A burst wave lithotripsy US transducer with an inline US imager was coupled to the flank and the lithotripter focus was aligned with the stone. Each stone was exposed to burst wave lithotripsy at 6.5 to 7 MPa focal pressure for 30 minutes under real-time image guidance. After treatment, the kidneys were removed for gross, histologic, and MRI assessment. Stone fragments were retrieved from the kidney to determine the mass comminuted to pieces <2 mm.
Results: On average, 87% of the stone mass was reduced to fragments <2 mm. In three of five treatments, stones were completely comminuted to <2-mm fragments. In two of five treatments, stones were partially disintegrated, but larger fragments remained. One stone was not treated because no suitable acoustic window was identified. No injury was detected through gross, histologic, or MRI examination in the parenchymal tissue, although petechial damage and surface erosion were identified on the urothelium of the collecting system limited to the area around the stone.
Conclusion: Burst wave lithotripsy can consistently produce stone fragments small enough to spontaneously pass by transcutaneous administration of US pulses. The data suggest that such exposures produce minimal injury to the kidney and urinary tract.

Keywords: shock wave lithotripsy, renal injury, burst wave lithotripsy, nephrolithiasis

Introduction

Burst wave lithotripsy (BWL) is an experimental modality that administers focused ultrasound (US) pulses to noninvasively break urinary tract stones. Whereas shock wave lithotripsy (SWL) delivers waves with a single compression/tension cycle[1] to fragment a stone, BWL can effectively disintegrate natural and artificial calculi *in vitro* using multicycle sinusoidal pulses. Characteristically, the size of fragments generated during BWL is controlled by the US frequency[2] and therefore BWL may reliably generate fragments small enough to asymptomatically and spontaneously pass through the urinary tract.

In previous experiments, a range of BWL exposures were delivered to porcine kidneys to assess for potential renal injury.[3] At higher pressure amplitudes, hemorrhagic injury similar to that observed in SWL sometimes occurred.[4,5] It was further demonstrated that the occurrence of renal injury correlates with the onset of sustained cavitation in the renal parenchyma, a phenomenon detected by real-time US imaging that suggests a role of cavitation in injury similar to SWL.

Based on these results, exposure parameters were identified that caused minimal renal injury, but were sufficient to disintegrate stones *in vitro*. The present study sought to assess stone fragmentation effectiveness and potential renal injury using these parameters in a pig model.

[1]Department of Urology, University of Washington School of Medicine, Seattle, Washington.
[2]Center for Industrial and Medical Ultrasound, Applied Physics Laboratory, University of Washington, Seattle, Washington.
[3]Department of Radiology, University of Washington School of Medicine, Seattle, Washington.
[4]Department of Anatomy and Cell Biology, Indiana University Purdue University at Indianapolis, Indianapolis, Indiana.
[5]Division of Urology, Department of Veterans Affairs Medical Center, Seattle, Washington.
A video demonstrating this technique is available online.

Methods

BWL system hardware

BWL exposures were delivered by a custom therapy transducer powered by an electric pulse generator developed in our laboratory. The transducer has an aperture of 85 mm and a central opening of 40×36 mm to accommodate a coaxially aligned imaging probe. The BWL transducer had a focal distance of 100 mm, creating an ellipsoidal focal volume with −6 dB dimensions of 60 mm along the acoustic axis and 6 mm transverse to the axis. The transducer was operated at 350 kHz to deliver 20-cycle pulses at a pulse repetition rate of 10 Hz, representing a duty factor of 0.057%.

A commercial US imager (Vivid E95 with M5Sc probe; GE Healthcare, Wauwatosa, WI) was used for targeting and real-time monitoring with B-mode and color Doppler imaging. Color Doppler is specifically useful for enhancing signal-to-noise ratios related to cavitation (both twinkling from the stone and cavitation elsewhere).[6–8] Imaging was not synchronized with the BWL system, but minimal interference was present because of the low therapy duty factor. Imaging was recorded by screen capture to a computer.

Porcine model

All procedures were approved by the University of Washington's Institutional Animal Care and Use Committee. Three female pigs weighing 70 to 80 kg each were used to assess stone fragmentation and renal injury from BWL. This pig model has a similar size and renal anatomy as humans and has been used in research on injury related to SWL and BWL.[9] On the day of the study, animals were sedated with 4 mg/kg tiletamine/zolazepam (Telazol; Zoetis, Parsippany, NJ) and maintained under a surgical plane of anesthesia with isoflurane. All animals were instrumented to monitor the heart rate, ECG, blood oxygen saturation, and temperature.

The abdomen of the animal was depilated and washed. A midline abdominal incision was made and a single human stone (6–7 mm) with a primary composition of calcium oxalate monohydrate was inserted into the renal pelvis or a calyx of each kidney through a small incision in the proximal ureter. Care was taken to avoid introducing air into the collecting space during insertion. Each stone was immersed in water for ≥1 week before implantation. Stone composition was predetermined by spectroscopic analysis, and all stones used were from a single patient. Before implantation, each stone was measured, weighed (wet), and photographed. After insertion, the incision in the proximal ureter was sutured closed, and the ureter lumen was partially constricted ($\sim 50\%$) using a suture to prevent loss of stone fragments. Although ureteral constriction may increase fluid in the kidneys, which can promote stone breakage,[10] no distention of the collecting space was noted. The location of the stone was variable; some stones were exposed in the renal pelvis with surrounding urine and some in calices with no surrounding fluid apparent on imaging. The abdominal cavity was filled with degassed saline to displace air and the abdominal incision was closed.

BWL treatment protocol

Stones were first imaged to determine a suitable acoustic window for BWL that would avoid obstacles, including ribs or bowel. A bath containing ~ 10 L of degassed water was prepared for acoustic coupling. The bath consisted of a plastic container with a hole in the bottom, lined by a 38-μm low-density polyethylene membrane. The skin was prepared by first wetting it with degassed water containing 1% isopropyl alcohol, then applying a layer of US gel that had been centrifuged to remove larger air bubbles. Degassed water was used to wet the surface of the gel layer before the coupling container was placed. The container was then filled with water, and air bubbles visible in the gel between the membrane and skin were removed. The therapy transducer and imaging probe were submerged in the water bath, held in place by a flexible mechanical arm.

US imaging was employed before exposure to align the focus with the stone and assess the acoustic window. Respiratory motion was present, but a targeting position could generally be achieved where the stone was in focus $\sim 75\%$ of the time or more. The transducer was rotated over a range of 180° about its axis to identify a clear acoustic window over the entire tissue path for the therapy transducer. All treatments involved BWL exposures lasting 30 minutes, delivered in 10-minute intervals. At the 10- and 20-minute marks, exposure was briefly paused to allow for realignment if necessary. This exposure regime was chosen to be similar to an SWL procedure, where retargeting is occasionally performed under fluoroscopic guidance. All treatments began by delivering BWL pulses at an output corresponding to focal peak negative pressure of 7 MPa measured in a free field. US imaging was monitored for cavitation occurring in the water bath or kidney parenchyma. Two signatures were used to detect cavitation: dynamic hyperechoic activity in the tissue with B-mode imaging[3] and twinkling artifacts indicative of bubbles using color Doppler.[6] If detected, treatment was paused for 60 seconds and then continued. If cavitation was still apparent, the output level was reduced to peak negative pressure of 6.5 MPa. Cavitation in the urine space around the stone on US imaging was considered normal (Supplementary Video S1).

Following treatment of both kidneys, the animal was euthanized. The midline abdominal incision was reopened for gross evaluation of the kidney and abdominal cavity in the acoustic path. The ureters as well as renal arteries and veins were ligated and kidneys were removed. The exteriors of the excised kidneys were cleaned, examined, and photographed, then transported for MRI within 2 hours. After MRI, kidneys were bivalved for recovery of stone fragments and gross examination of the collecting space. Within 3 hours after treatment, kidneys were fixed in 10% neutral buffered formalin for histopathological evaluation.

Recovered fragments were sieved through serial mesh filters. All stone pieces that passed through a 2-mm sieve were considered fully comminuted. Remaining larger fragments were weighed wet and compared with the original stone weight to determine the fraction of mass disintegrated for each stone. Image analysis of the fragment size distribution was conducted from photographs converted to binary images by thresholding using Otsu's method.[11] The equivalent diameter of each fragment was calculated from the area as $D_{eq} = \sqrt{4 \times area/\pi}$.

Histologic characterization of renal lesions

Tissue samples were taken from the location where the stone was targeted based on US imaging and processed for

Table 1. Stone Dimensions and Weights Before Implantation and After Treatment

Stone	Initial mass (mg)	Size (mm)	Remaining mass >2 mm (mg)	Remaining mass >4 mm (mg)	% Fragmented <2 mm	% Fragmented <4 mm
1[a]	74	6×3×3	0	0	100	100
2	82	7×5×4	0	0	100	100
3	124	7×7×5	52	52	58	58
4	60	6×3×3	0	0	100	100
5[a]	162	7×5×5	38	0	77	100
Average	100±37		18±22	10±21	87±17	92±17

[a]Cavitation in tissue occurred during treatment.

histological evaluation. During the preparation for histological processing, the kidney was evaluated for signs of tissue injury within the parenchyma. Serial sections were stained with a hematoxylin and eosin stain and periodic acid–Schiff stain.[12] A blinded examination of slides was performed by an expert in SWL kidney injury (J.C. Williams Jr.).

MRI of excised kidneys

MRI techniques have been recently developed to quantify hemorrhagic injury to kidneys related to lithotripsy.[3,13] *Ex vivo* MRI was performed on all treated kidneys. Turbo spin-echo (TSE) T1-weighted (recycle time [TR]/echo time [TE] = 633/23 ms) and T2-weighted (TR/TE = 7990/75 ms) imaging, as well as gradient-echo-based susceptibility-weighted (TR/TE = 14.7/20.8 ms) imaging, was performed using a 3-Tesla MRI scanner (Ingenia; Philips Healthcare, Best, The Netherlands). T1-weighted and T2-weighted TSE imaging sequences were performed with 156-μm in-plane resolution and 1-mm slice thickness; susceptibility-weighted imaging was performed with 450-μm in-plane resolution and 2-mm slice thickness.

Each slice was evaluated for injury within the parenchyma, as described previously.[3] Susceptibility-weighted imaging and additional T1-weighted (TR/TE = 178/2.4 ms, flip angle = 3°) gradient-echo imaging were conducted to first identify injured regions and examine sample positions. TSE T1-weighted and T2-weighted images were compared with correlate injured regions within the kidney.

Results

Stones were implanted in all six kidneys. However, treatment was administered in only five kidneys because the acoustic window was too small to ensure delivery of energy in one case. The remaining five underwent 30 minutes of BWL exposure. The skin-to-stone depth ranged between 5.4 and 6.1 cm. During exposure, cavitation was observed on B-mode US in the urine around each stone. In two cases, cavitation was also observed in kidney tissue at treatments of 7 MPa (Table 1). In one case, treatment was resumed at 7 MPa and no further cavitation was detected. In the other case, after reducing the pressure amplitude to 6.5 MPa, no tissue cavitation was observed.

An average 87% (minimum 58%) of the mass was comminuted to fragments <2 mm in the five treatments (Table 1). In three of the five experiments, the stone was completely disintegrated (Table 1). In the remaining two experiments (which included the two largest stones by mass), fragments >2 mm were present post-BWL (Fig. 1). In one case, this was represented by a large remaining stone fragment (~6×3 mm), while in the other, two 2.5- to 3-mm fragments were present after treatment. Many fragments in the range of ~1 to 2 mm were recovered in each treatment (Figs. 1 and 2), and fine dust too small to collect was also present.

Gross examination of kidneys revealed minor petechial hemorrhage to the urothelium in the collecting space immediately surrounding the area containing a majority of the stone fragments (Fig. 3). No bleeding, hematoma, or other injury was observed on the capsular surfaces of any kidney.

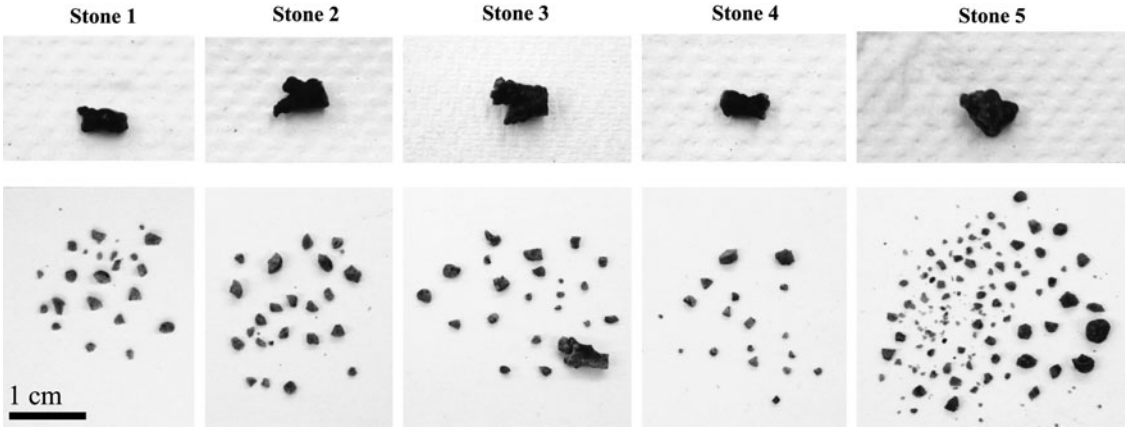

FIG. 1. Photographs of all stones before implantation (*top*) and fragments extracted after 30-minute BWL exposures (*bottom*). BWL = burst wave lithotripsy.

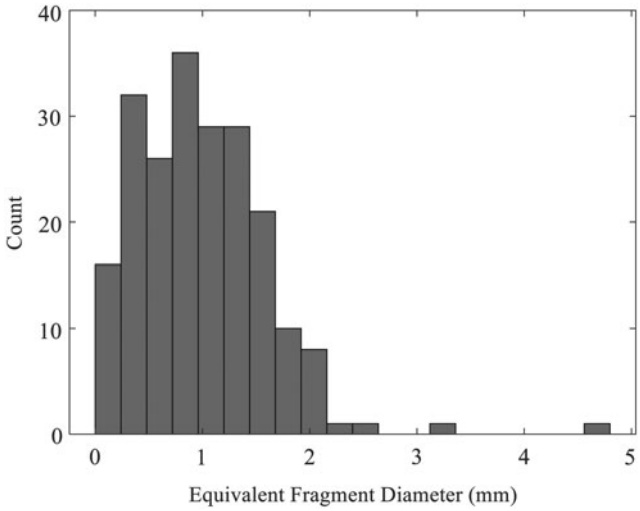

FIG. 2. Distribution of sizes for 211 fragments recovered from the five treatments, as calculated by image analysis. Nearly all fragments have <2 mm equivalent diameter.

No indications of damage to the skin overlying the treatment site or intervening tissues were observed upon inspection.

Histology showed damage to the collecting space mucosa around the stone (Fig. 4). Damage ranged from epithelial sloughing with small focal hemorrhagic spots to larger hemorrhagic regions extending through the full thickness of the lamina propria. Damage was limited to an area similar to the width of the US focus and stone ($\sim$1 cm diameter). No damage in the renal parenchyma was observed by histology for any experiment. MRI likewise indicated no discernable injury in fresh and fixed kidney parenchyma. Stone fragments were visible on MRI within the collecting space (Fig. 5).

Discussion

BWL has been previously investigated *in vitro* for stone fragmentation and *in vivo* for tissue injury to kidneys without stones.[2,3] The present study describes a first demonstration treating renal stones with BWL in an animal model. BWL may be a useful first-line technology for fragmenting urinary stones and has several potential benefits, including predictable and consistent fragment sizes, effectiveness for a variety of stone types, and low-pressure amplitudes that limit kidney injury.

In this study, we found that BWL fragmented all treated stones with an average of 87% of the stone mass reduced to <2-mm fragments and three of five stones completely comminuted. We used a 350-kHz transducer, which primarily generated fragments from submillimeter dust to 2 mm. One treatment did not comminute a large piece of the original stone representing 42% of the mass, while the other incomplete treatment left two $\sim$3-mm fragments. These cases also contained the largest stones by mass, and BWL appears to proceed at a linear rate of stone fragmentation,[14] indicating that larger stones may require extended treatment for a set of parameters. It is also possible that these portions of the stones were not targeted throughout the entire treatment, underscoring a need for effective monitoring of treatment endpoint.

We found injury to the kidney only in the immediate vicinity of the stone, limited to surface layers of the collecting system. This superficial injury did not extend to parenchymal tissues as MRI analysis and histology did not reveal any morphological anomalies to kidney parenchyma in the treatment path. The MRI method utilized high-resolution scans of the kidney as previously validated for detection and quantification of hemorrhagic renal injury in both SWL[13] and BWL.[3] Cavitation in tissue was detected in two treatments, but was brief (<65 seconds); resolved with our countermeasures; and did not translate to any attributable parenchymal injury. This compelling result suggests that US imaging feedback to detect cavitation may help prevent injury by allowing the operator to temporarily pause and adjust the treatment parameters to spare renal tissue. However, further functional studies are needed to determine whether BWL has any reversible or irreversible impact on renal function. We cannot rule out the possibility that the two kidneys treated after a preceding contralateral treatment benefitted from a pretreatment protective effect, thought to occur through vasoconstriction in SWL.[15]

The porcine model has been employed in numerous studies of SWL-induced injury,[9,16] but the effectiveness of lithotripters is usually evaluated *in vitro*. However, our experiments suggest that many *in vitro* studies do not replicate important factors for stone breakage *in vivo*, including urine

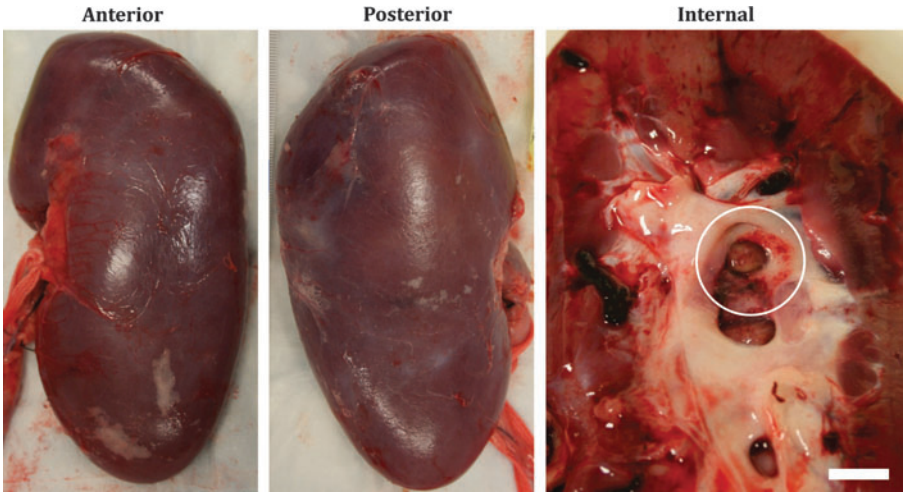

FIG. 3. Typical gross appearance (left, anterior, and center, posterior) of a freshly excised kidney exposed to 30-minute BWL treatment, showing no apparent injury to the capsular surface, but petechial injury to the urothelium (circular outline in right image), in the vicinity of stone fragments. The scale bar in the right image is 1 cm.

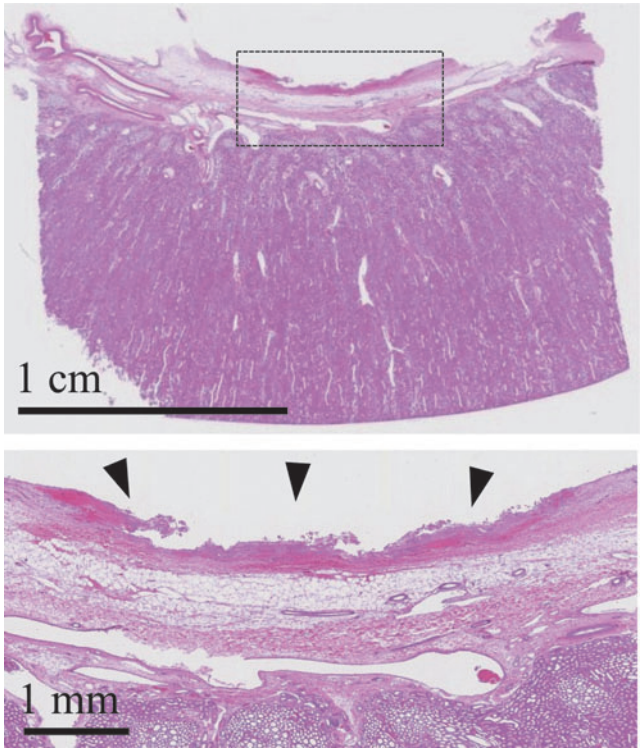

FIG. 4. Hematoxylin and eosin histology slide showing a section distal to an exposed stone in the kidney. The *bottom slide* is a magnified view of the area outlined in the *top slide*. Focal mucosal injury is observed in the location of treatment (*arrowheads*), extending to the lamina propria of the wall, but not into the renal parenchyma.

gas concentration and fluid confinement.[17] As such, we felt it important to develop a porcine model using human stones without altering the collecting system or renal parenchyma. While this model allowed consistent stone treatment and injury evaluation, there are ways in which it does not replicate a clinical scenario. Pigs have a large rib cage that extends further inferior than humans and limits the acoustic window. Pig kidneys are also partially intraperitoneal and thus the impact of intestine is more problematic than would be expected in humans. To address this issue, we carefully checked the acoustic window using US imaging to ensure that these structures did not overlap the converging focused therapy beam. Artifacts in the US image were valuable indications of acoustic obstruction, and in one case, we chose not to treat a stone because no suitable window was identified. We also limited the stones to a size that is clinically relevant, but no larger than the focal beam, and limited them to a single composition, although one that is considered more difficult to fragment in SWL.[18] In humans, stone compositions have varying fragility and will require different doses to fragment. In preliminary *in vivo* experiments developing the animal model, we similarly found variability in stone fragmentation and identified stone composition as a potential cause. By careful control of factors affecting therapy delivery, we have been able to demonstrate consistent stone fragmentation.

Some challenges remain in translating the methods here to clinical use. We chose a 30-minute treatment based on preliminary *in vitro* and *in vivo* data. We chose 6- to 7-mm stones as these are clinically relevant and similar to the specific transducer focal width; simulations and data suggest that a focus broader than the stone is more effective in achieving comminution with SWL.[19] More research is needed to determine an appropriate BWL exposure time based on stone size and composition. In addition, the skin-to-stone distance is a known predictor of SWL outcomes,[20] which could have effects on targeting and delivery of the US to the target stone in larger patients. Even in the present model, it can be difficult to identify and target all fragments of the stone as well as define a clear endpoint solely through two-dimensional US imaging, although preliminary data suggest that ultrasonic propulsion can separate a group of fragments to differentiate intact and disintegrated stones.[21] This challenge may explain the difficulty achieving complete comminution in two stones. Our coupling method, which allowed visual inspection for bubbles, may also not be practical in a modern clinical setting. It is more likely that a clinical BWL transducer would be coupled either directly or by a water bolus to the patient's skin.

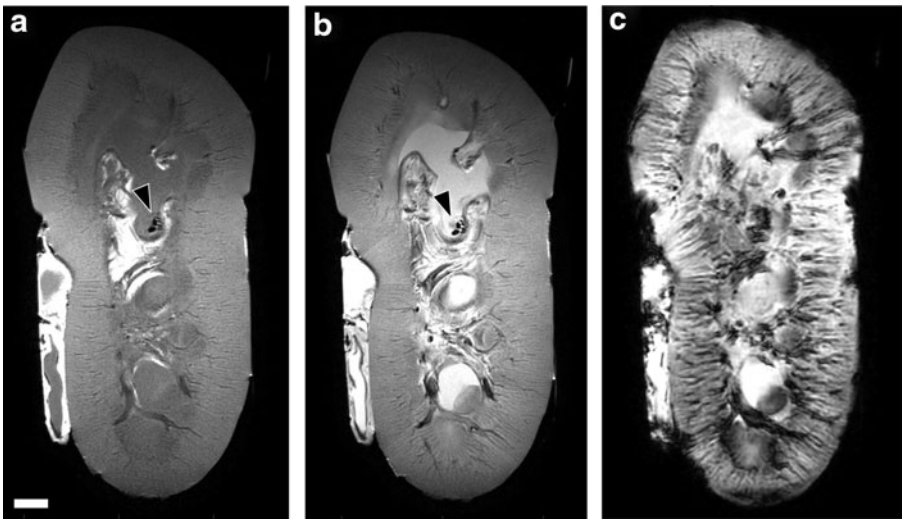

FIG. 5. MRI appearance of renal tissue in freshly excised kidneys. **(a–c)** Sample image slices show locations of stone fragments (*arrowheads*), but no apparent hemorrhagic injury using the T1-weighted TSE image **(a)**, T2-weighted TSE image **(b)**, and susceptibility-weighted image **(c)**. Scale bar = 1 cm. TSE = turbo spin-echo.

Conclusion

We developed and implemented an animal model to perform clinical simulation of BWL to noninvasively fragment kidney stones. The results indicate that BWL can produce consistent fragmentation of urinary stones of a clinically relevant size in the kidney while avoiding detectable injury to functional renal tissue.

Acknowledgments

The authors thank Christopher Hunter, Jeff Thiel, Barbrina Dunmire, and Jessica Dai for assistance with experiments and NASA Exploration Medical Capabilities for providing the flexible ultrasound system (imager) used in this study. They also acknowledge financial support from NIH through NIDDK P01 DK043881 and K01 DK104854 and from resources through the VA Puget Sound Health Care System, Seattle, Washington.

Author Disclosure Statement

A.D.M., B.W.C., M.R.B., and M.D.S. have equity in and consulting agreements with SonoMotion, Inc., which has licensed technology related to this work from the University of Washington.

Funding Information

No funding was received for this article.

Supplementary Material

Supplementary Video S1

References

1. Cleveland RO, McAteer JA. Physics of shock-wave lithotripsy. In: Arthur D. Smith MD, Gopal H. Badlani MD, Glenn M. Preminger MD, Louis R. Kavoussi MD. Smith's Textbook of Endourology. Hoboken, NJ: Wiley-Blackwell, 2012, pp. 527–558.
2. Maxwell AD, Cunitz BW, Kreider W, et al. Fragmentation of urinary calculi in vitro by burst wave lithotripsy. J Urol 2015;193:338.
3. May PC, Kreider W, Maxwell AD, et al. Detection and evaluation of renal injury in burst wave lithotripsy using ultrasound and magnetic resonance imaging. J Endourol 2017;31:786.
4. McAteer JA, Evan AP. The acute and long-term adverse effects of shock wave lithotripsy. Semin Nephrol 2008;28: 200.
5. Bailey MR, Pishchalnikov YA, Sapozhnikov OA, et al. Cavitation detection during shock-wave lithotripsy. Ultrasound Med Biol 2005;31:1245.
6. Li T, Khokhlova TD, Sapozhnikov OA, et al. A new active cavitation mapping technique for pulsed HIFU applications—Bubble Doppler. IEEE Trans Ultrason Ferroelectr Freq Control 2014;61:1698.
7. Lu W, Sapozhnikov OA, Bailey MR, et al. Evidence for trapped surface bubbles as the cause for the twinkling artifact in ultrasound imaging. Ultrasound Med Biol 2013;39: 1026.
8. Sorensen MD, Harper JD, Hsi RS, et al. B-mode ultrasound versus color Doppler twinkling artifact in detecting kidney stones. J Endourol 2013;27:149.
9. Blomgren PM, Connors BA, Lingeman JE, et al. Quantitation of shock wave lithotripsy-induced lesion in small and large pig kidneys. Anat Rec 1997;249:341.
10. Holmer NG, Almquist LO, Hertz TG, et al. On the mechanism of kidney stone disintegration by acoustic shock waves. Ultrasound Med Biol 1991;17:479.
11. Otsu N. A threshold selection method from gray-level histograms. IEEE Trans Syst Man Cybern 1979;9:62.
12. McManus JF. The periodic acid routing applied to the kidney. Am J Pathol 1948;24:643.
13. Handa RK, Territo PR, Blomgren PM, et al. Development of a novel magnetic resonance imaging acquisition and analysis workflow for the quantification of shock wave lithotripsy-induced renal hemorrhagic injury. Urolithiasis 2017;45:507.
14. Zwaschka TA, Ahn JS, Cunitz BW, et al. Combined burst wave lithotripsy and ultrasonic propulsion for improved urinary stone fragmentation. J Endourol 2018;32:344.
15. Handa RK, Bailey MR, Paun M, et al. Pretreatment with low-energy shock waves induces renal vasoconstriction during standard shock wave lithotripsy (SWL): A treatment protocol known to reduce SWL-induced renal injury. BJU Int 2009;103:1270.
16. Matlaga BR, McAteer JA, Connors BA, et al. Potential for cavitation-mediated tissue damage in shock wave lithotripsy. J Endourol 2008;22:121.
17. Ahn J, Kreider W, Hunter C, et al. Improving environmental and stone factors toward a more realistic in vitro lithotripsy model. J Acoust Soc Am 2017;141:3673.
18. El-Nahas AR, El-Assmy AM, Mansour O, et al. A prospective multivariate analysis of factors predicting stone disintegration by extracorporeal shock wave lithotripsy: The value of high-resolution noncontrast computed tomography. Eur Urol 2007;51:1688.
19. Qin J, Simmons WN, Sankin G, et al. Effect of lithotripter focal width on stone comminution in shock wave lithotripsy. J Acoust Soc Am 2010;127:2635.
20. Perks AE, Schuler TD, Lee J, et al. Stone attenuation and skin-to-stone distance on computed tomography predicts for stone fragmentation by shock wave lithotripsy. Urology 2008;72:765.
21. Harper JD, Cunitz BW, Dunmire B, et al. First in human clinical trial of ultrasonic propulsion of kidney stones. J Urol 2016;195:956.

Address correspondence to:
Adam D. Maxwell, PhD
Department of Urology
University of Washington School of Medicine
1013 NE 40th Street
Seattle, WA 98105

E-mail: amax38@uw.edu

Abbreviations Used

BWL = burst wave lithotripsy
MRI = magnetic resonance imaging
SWL = shock wave lithotripsy
TE = echo time
TR = recycle time
TSE = turbo spin-echo
US = ultrasound